

# ***A MEMS-Based High-Sensitivity & Speed Ionization Sensor for Multi-parameter Bioaerosol Monitoring***

**Yiming Li**

*School of Physics and Astronomy, University of Glasgow, Glasgow, United Kingdom*  
*lym\_cdbd@outlook.com*

**Abstract.** In areas such as respiratory disease prevention and control, life science research, and food and drug development, bioaerosol samplers can monitor the surrounding environment in real time. Within bioaerosol research, various gas sensor designs have been developed based on different collection principles, including liquid impaction, solid impaction, cyclone, filtration, and electrostatic methods. However, due to the diverse characteristics of bioaerosols, instruments employing different design principles show variations in physical and biological sampling efficiency for different bioaerosol particles. The objective of this paper is to examine the design of a highly sensitive, high-speed microelectromechanical systems' (MEMS) electrode ionization bioaerosol gas sensor. This study investigates the sensitivity characteristics of gas sensors toward aerosols, with the aim of improving upon the limitations of existing gas sensor designs. First, a silicon micropillar sensor composed of a three-electrode structure is proposed for real-time monitoring of multiple parameters, including particulate matter concentration, gas concentration, and temperature. Second, the sensing mechanism of the silicon micropillar toward particulate matter, gas, and temperature is explored. The analysis is based on gas discharge, field-assisted emission, and particle charging theories, establishing a direct detection principle for these parameters. Finally, experiments and simulations were conducted to investigate the effects of micropillar aspect ratio and electrode spacing on sensor performance and bioaerosol sensitivity.

**Keywords:** Bioaerosols, MEMS, Ionization, Silicon Micropillar, Sensor.

## **1. Introduction**

Recent advances in microelectromechanical systems (MEMS) have enabled the development of miniaturized, low-power sensors for rapid environmental detection. MEMS-based ionization sensors, which utilize enhanced electric fields from nanostructures, provide high sensitivity and fast response in gas monitoring [1]. However, their application to bioaerosol detection remains limited, and the effects of microstructural parameters such as aspect ratio and electrode spacing on sensing performance are not fully understood [2].

To overcome the above limitations, this study proposes a high-sensitivity and high-speed MEMS electrode ionization gas sensor for bioaerosol monitoring. The system employs a silicon micropillar-based three-electrode structure. It enables simultaneous detection of particulate matter, gas

concentration, and temperature. Based on gas discharge theory, field-assisted emission, and particle charging mechanisms, the sensing principle was investigated through both simulation and experimental analysis. In addition, sensors with chromium micropillars of different geometries were used to evaluate sensitivity to bioaerosols. Particular attention was paid to the effects of aspect ratio and electrode spacing.

This work aims to deepen the understanding of ionization-based MEMS sensing mechanisms. It also provides a foundation for integrated, miniaturized, and real-time bioaerosol monitoring systems.

## 2. Related works

Bioaerosols consist of airborne microorganisms and biological fragments, such as bacteria, fungi, viruses, and pollen. They are widely present in both natural and built environments. These particles are a major source of air pollution and are associated with various health issues, including infectious diseases, allergies, and chronic respiratory disorders [3]. Due to their small aerodynamic size, many bioaerosol particles can penetrate deep into the respiratory tract and reach the alveolar region. This poses a significant health risk [4]. These findings highlight the urgent need for real-time and high-sensitivity monitoring technologies [5].

Various bioaerosol sampling methods have been developed to improve collection efficiency and preserve microbial viability. Liquid impingement captures airborne particles into a liquid medium, which helps maintain biological activity. However, this method is susceptible to dilution and evaporation effects [6]. Cyclone separation uses centrifugal forces for continuous, high-flow sampling, but its effectiveness for submicron particles is limited. In contrast, electrostatic sampling charges and collects particles using an electric field. This enables a gentle, efficient, and low-pressure-drop collection process [7]. Despite these advantages, the physical and biological collection efficiencies of each method vary with particle size, charge, and humidity. This variability limits their suitability for real-time detection.

## 3. Methodology

This article focuses on the simulation of the characteristics of a silicon micropillar three-electrode sensor, the experimental investigation of its sensitivity, and the detection of multiple parameters. The main research objective is to establish a technical approach for the direct analysis of bioaerosols, thereby advancing core technologies such as the silicon micropillar three-electrode sensor, weak alternating current (AC) detection, and intelligent data processing and analysis modules. Highly sensitive digital bioaerosol detection has been achieved through system integration and software development.

### 3.1. Physical modeling and control equations of silicon micropillar three-electrode sensor

COMSOL Multiphysics was used to develop a three-dimensional multiphysics model of the silicon micropillar three-electrode sensor. The model employs high-aspect-ratio silicon micropillars as its core structure, forming a typical three-electrode ionization sensor geometry through coaxial or parallel arrangement of the emitter, gate, and collector electrodes. Geometric parameters—including pillar diameter  $d$ , pillar height  $h$ , pillar spacing  $p$ , and electrode spacing  $g$ —were set as variables in the simulation to analyze the influence of structural dimensions on electric field distribution, ion transport, and collection characteristics. The dielectric region adopts the equivalent parameters of air

or carrier gas, with effective ionization and recombination coefficients defined, and a direct current (DC) or weak AC bias applied at the electrode boundaries. The inlet boundary specifies the initial ion or aerosol particle concentration and flow rate, while the wall applies non-flux or surface composite boundary conditions to ensure physical consistency in the transport process. The following sensor physical models are considered in sequence: gas particles and chemical reactions, field governing equations, initial and boundary conditions, and mesh components.

The electric field distribution inside the sensor satisfies Poisson's equation

$$\nabla \cdot (\varepsilon \nabla \varphi) = -\rho, \quad (1)$$

the ion transport process is governed by the drift-diffusion continuity equation, which is given by

$$\frac{\partial n}{\partial t} + \nabla \cdot J = R, \quad (2)$$

and the flux expression is given by

$$J = \pm q\mu n \nabla \varphi - D \nabla n, \quad (3)$$

where  $\varepsilon$  is the permittivity of the material,  $\varphi$  is the electric potential,  $\rho$  is the charge density,  $n$  is the ion concentration,  $t$  is time,  $R$  is the net generation-recombination rate,  $\mu$  is the mobility, and  $D$  represents the diffusion coefficient.

For charged aerosol particles, a drift-diffusion-convection coupling model is introduced to describe their trajectory and collection probability under the influence of electric field, Brownian diffusion, and background airflow. The ion balance and particle charging dynamics are described using classical ion-particle interaction rate equations derived from aerosol charging theory, as shown in equation (4-7). In the absence of particles, the ion concentration decreases mainly due to ion-ion recombination, which can be expressed as

$$\frac{dn_i^{wo}(t)}{dt} = -\alpha [n_i^{wo}(t)]^2, \quad (4)$$

where

$$\alpha = \frac{z_i e}{\varepsilon_0}, \quad (5)$$

is the ion recombination coefficient,  $z_i$  is the ionic charge number,  $e$  is the elementary charge, and  $\varepsilon_0$  is the vacuum permittivity.

When particles are present, ions are additionally consumed by ion-particle attachment during the particle charging process. The ion balance equation is given by

$$\frac{dn_i^w(t)}{dt} = -\alpha[n_i^w(t)]^2 - \frac{dq_p(t)}{dt} n_p(t), \quad (6)$$

where  $n_p(t)$  denotes the particle number concentration and  $q_p(t)$  represents the average particle charge.

The time evolution of the number concentration of particles carrying  $q$  elementary charges is governed by

$$\frac{dn_p^{(q)}(t)}{dt} = \beta_{(q-1)} n_p^{(q-1)}(t) n_i^w(t) - \beta_q n_p^{(q)}(t) n_i^w(t), \quad (7)$$

where  $\beta_q$  is the ion-particle attachment coefficient for particles with charge state  $q$ .

This type of coupling model has been widely used in nano-scale ion migration and electrochemical sensing simulations [8,9], effectively capturing the field concentration effect and particle collection dynamics at the electrode tip. For sensors with different electrode spacings, the influence of current density is modeled and simulated, focusing on the effect of different electrode spacings on the sensor's collection current density.

### 3.2. Simulation solution and parameter setting

During simulation, the mesh was refined in the electrode tip and inter electrode gap regions to accurately capture the sharp variations in electric field and concentration gradients. A combined steady state and transient solution strategy was adopted: the electric field equations were solved under steady state conditions, followed by iterative solution of the ion transport equations in the time domain until convergence was achieved. The finite volume method was used for discretization, together with adaptive step size control and a convergence residual criterion to ensure numerical stability. The primary outputs of interest are the cathode current density  $J_c$ , the average positive ion density  $n_+$  between the electrodes, and the collector current density  $J_{col}$  [10]. These metrics are used to evaluate sensing performance under different structural parameters. A simulation comparison was conducted using silicon micropillar three-electrode sensors with a low aspect ratio that had been used in earlier studies to analyze the cathode current density, inter-electrode positive ion density, and collector current density. Results indicate that higher inter electrode positive ion density, cathode current density, and collector current density correspond to improved discharge characteristics and superior sensor performance.

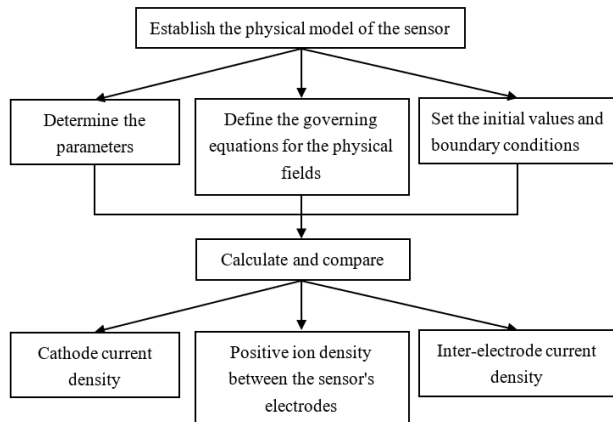


Figure 1. Flowchart of sensor simulation and performance analysis based on physical fields

The following discussion focuses on the modeling and simulation process of the above model, as illustrated in Figure 1. The electrostatic field module, charged particle tracking module, and plasma module in COMSOL Multiphysics software are used to simulate the potential distribution of the silicon micropillar three-electrode sensor, the motion of charged particles within the sensor, and the gas discharge process between the electrodes, respectively, thereby achieving the simulation model of the sensor as shown in Figure 2.

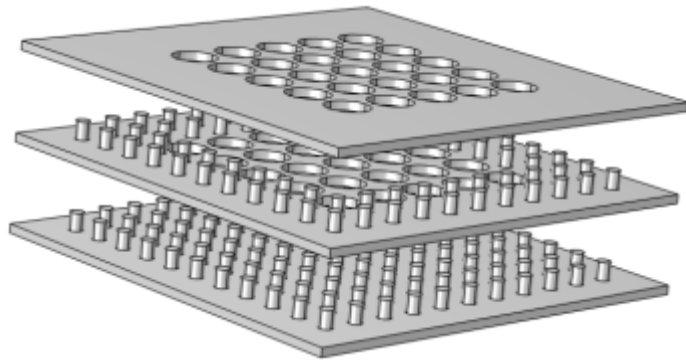


Figure 2. Three-dimensional model of the silicon micropillar three-electrode sensor

It should be noted that the silicon micropillar three-electrode sensor in this study enables the detection of particulate matter concentration, gas concentration, and temperature through measurement of the sensor collection current. The collection electrode current consists of the ion flow generated by gas discharge and the current produced by the motion of charged particles, as shown in equation (5). The formation of the sensor collection current is a multiphysics process, involving gas discharge, ion charging upon collision with particles, and the motion of charged particles and ions under various fields.

In summary, the fourth chapter of this paper focuses on analyzing the formation process of the sensor collection current and performing accurate numerical simulations of each physical process. The sensor physical model is constructed, primarily comprising the gas discharge electric field model, the particle motion model, and the particle charging model.

### 3.3. High-sensitivity & speed MEMS three-electrode ionization bioaerosol sensor

The main technical challenges currently hindering the advancement of bioaerosol detection are the insufficient sensitivity, slow response speed, and significant signal-noise interference of single-electrode or low-aspect-ratio ionization sensors. Furthermore, these sensors lack stable recognition capabilities in complex multi-parameter environments. To overcome these limitations, this study proposes a high-sensitivity, high-speed MEMS three-electrode ionization sensor design based on a multi-faceted silicon micropillar structure, building upon the aforementioned physical model and electric field simulation. This design aims to achieve synergistic improvements in ionization efficiency, stability, and response speed through structural optimization, electrode parameter control, and intelligent signal processing, thereby enabling real-time simultaneous detection of multiple parameters such as particulate matter, gas concentration, and temperature.

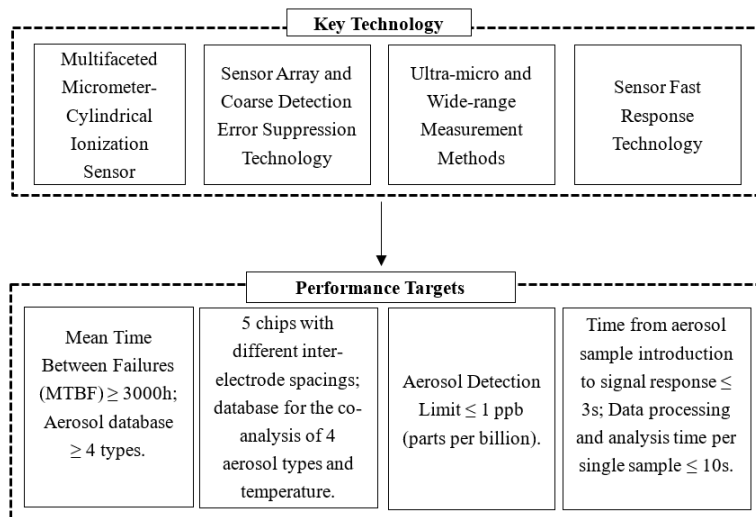


Figure 3. Research roadmap for the high-sensitivity, high-speed MEMS three-electrode ionization bioaerosol sensor

Through experiments on the sensitivity of the sensor to microbial species, concentration, and particle size in bioaerosols, a sensor model is established by integrating data fusion techniques with sensor outputs. This approach allows for the simultaneous detection of microbial species, concentration, and particle size in bioaerosol particles. The research roadmap for this section is illustrated in Figure 3.

#### 3.3.1. Multifaceted micrometer-cylindrical ionization sensor

First, to achieve high-sensitivity detection and rapid response for bioaerosols, this study optimized the structural parameters of a multi-faceted micropillar three-electrode ionization sensor. The sensor's core consists of an emitter, a grid, and a collector. The local electric field distribution between the emitter and the grid directly affects ionization efficiency and sensitivity. The thickness of the metal film deposited on the silicon micropillar can be adjusted to regulate the enhancement of the local electric field. The metal film thickness should be kept within 100–200 nm to ensure optimal conductivity and stability [11]. If the film is too thick, parasitic capacitance will be introduced, which can degrade sensor performance. Conversely, if the film is too thin, electrode inhomogeneity may occur.

Secondly, experiments were conducted to compare the sensitivity of silicon micropillar three-electrode sensors with different aspect ratios to bioaerosol particles, in order to establish an optimal electrode spacing range that balances performance and stability for high-aspect-ratio sensors. Additionally, the performance of high-aspect-ratio sensors was examined in comparison with that of low-aspect-ratio silicon micropillar three-electrode sensors.

These optimizations enable the sensor to meet the longterm stability requirement of a mean time between failures (MTBF)  $\geq 3000$  hours [12]. Additionally, to allow singlevalue response identification of different aerosol particle types (such as bacterial spores, pollen, and dust), parameters including pulse voltage amplitude, frequency, and duty cycle were further adjusted to achieve efficient aerosol sampling and accurate identification.

### 3.3.2. Ionization sensor array and coarse detection error suppression technology

Based on unit-level optimization principles, a multi-channel ionization sensor array system was developed. The array consists of five groups of micron-scale three-electrode chips with different electrode spacings. Each chip group can independently adjust its bias voltage and sampling period, enabling coordinated responses to aerosol particle characteristics under multi-scale electric field conditions. The array is capable of simultaneously measuring multiple parameters, including particulate concentration, gas composition, and temperature. In addition, it supports aerosol classification and concentration analysis using multi-dimensional datasets. This approach allows the construction of a database for the coordinated analysis of four aerosol types under varying temperature conditions. Specifically, experiments were conducted using chromium-based micron-scale sensors with different electrode spacings to investigate the correlation between electrode spacing, collected current, and responses to changes in multiple physical parameters.

Furthermore, an array composed of eight silicon-based micron-scale three-electrode sensors with different electrode spacings was used to perform sensitivity measurements on bioaerosol particles. These experiments investigated the sensor responses to variations in microorganism type, concentration, and particle size. Quantitative analysis was carried out to determine the sensitivity of the sensors to target measurement parameters, and different electrode spacings were employed to evaluate overall sensor performance.

To address issues such as environmental noise, non-uniform ionization, and signal drift, a neural-network-based (NN-based) coarse detection error suppression algorithm was proposed. This algorithm automatically identifies and removes anomalous data by real-time comparison of the time-domain and frequency-domain characteristics of signals from each channel in the array. As a result, data stability and accuracy are significantly improved. Using this method, the sensor array achieves reduced measurement error, provides higher precision for subsequent bioaerosol concentration analysis, and supports the establishment of a database containing at least four types of aerosols [11].

### 3.3.3. Ultra-micro and wide-range measurement methods

To meet the detection requirements for bioaerosols at exceptionally low concentrations, this study investigated ultra micro and wide range detection methods both theoretically and experimentally. It is theoretically possible to resolve current signals at the sub microampere level by optimizing the geometry of the ionization region and the bias voltage, thereby lowering the detection limit. Furthermore, an adaptive range extension mechanism was designed to dynamically adjust the ionization voltage and sampling period, ensuring that the output signal maintains a linear relationship across a wide concentration range.

To achieve the target aerosol detection limit of 1 part per billion (ppb) [13], a highly sensitive ionization and ion collection method was employed to enable accurate detection of aerosol particles even at ultra-low concentrations. Considering the dynamic fluctuations in aerosol concentration, this study also proposes an adaptive range adjustment strategy to prevent signal saturation in high concentration environments while maintaining stability in low concentration conditions.

### 3.3.4. Sensor fast response technology

In highly dynamic environments, the concentration and composition of bioaerosols change rapidly. Therefore, the sensor response time is a critical performance metric. To meet the required response time, this study optimized the thickness of the metal layer on the silicon-based electrode surface. The response time is defined as the interval between sample introduction and the onset of the signal response. Increasing the metal layer thickness improves charge conductivity and reduces electrode resistance, which accelerates the signal response.

In addition, enlarging the electrode contact area and reducing the electrode spacing enhance the electric field strength. This shortens the ion migration and collection paths. The optimized sensor structure significantly improves the response speed and generates a detectable signal within three seconds after aerosol introduction [14]. Moreover, the processing time for a single data sample remains below 10 seconds, which meets the requirements for real-time monitoring [15].

To further improve temporal resolution and data throughput, a multi-channel parallel sampling scheme combined with data buffering was implemented. This configuration allows rapid switching between different measurement ranges and supports real-time data analysis during dynamic monitoring. As a result, the total processing and analysis time for each sample is maintained within 10 seconds. Finally, an artificial neural network was used to evaluate the fast-response performance of the sensor system. The aim was to verify that the maximum reference error in identifying bioaerosol microorganism type, particle size, and concentration remains below 10%.

## 4. Experiments

### 4.1. Direct analysis techniques for key scientific issues of bioaerosols

Studying the chemical composition and identification mechanisms of bioaerosols is critical for the prevention and treatment of respiratory diseases. A highly stable and sensitive detection method for bioaerosols is essential to ensure the safe monitoring of trace bioaerosols in the pharmaceutical and food industries. The mechanism for direct aerosol analysis plays a key role in determining the time required for aerosol analysis and testing. Conventional bioaerosol analysis techniques typically require aerosol particle sampling followed by image analysis, which cannot achieve highly stable and sensitive detection of bioaerosols.

Therefore, this chapter successfully confirms the chemical composition of bioaerosols and explores a highly stable and sensitive detection approach using an ionization three-electrode sensor.

### 4.2. Key technical issues

#### 4.2.1. Field-induced ionization bioaerosol direct analysis and testing technology

Gas molecules are ionized and charged through field-induced charging and diffusion charging mechanisms. This occurs via the physical adsorption of gas molecules onto bioaerosol particles,

thereby imparting a charge to the particles. The amount of charge carried by different aerosol types is related to their molecular structure.

The charged bioaerosol particles are accelerated by the electric field between the lead-out and collection electrodes of the three-electrode system and are collected by the collection electrode. This process produces an output current that follows a single valued relationship with aerosol concentration, enabling the direct detection of bioaerosol concentration. Research on signal acquisition and data analysis methods will be carried out to achieve synergistic analysis and testing of bioaerosol types and concentrations.

In summary, field induced ionization bioaerosol direct analysis and testing technology is identified as the key technical challenge addressed in this chapter.

#### **4.2.2. High-sensitivity & speed MEMS three-electrode ionization aerosol sensor**

The three-electrode aerosol sensor is the core component of the instrument, and its performance directly determines the overall system performance. Effectively addressing the issues of low sensitivity and slow response is crucial for developing high-speed, high-sensitivity aerosol sensors. Sensors with varied electrode spacings serve as the key elements for the simultaneous detection of four aerosol types and temperature. Resolving the challenge of separating these four aerosol types while concurrently detecting temperature is essential for achieving high-sensitivity, high-speed aerosol detection and analysis using the sensor.

In summary, the high-sensitivity, high-speed MEMS three-electrode ionization aerosol sensor technology represents one of the key technical challenges addressed in this chapter.

### **4.3. Results**

#### **4.3.1. Modeling results**

The performance of the MEMS aerosol sensor is a core component that significantly influences the entire instrument. To achieve a high-precision, high-reliability, long-life ionization-type bioaerosol sensor, it is crucial to resolve key MEMS fabrication challenges for the electrodes. Specifically, structural parameters such as the electrode surface metal layer thickness and the inter-electrode spacing must be tightly controlled to meet the design specifications. The structure is shown in Figure 2.

Simulation results demonstrate that the ionization-type aerosol MEMS sensor generates a micro current signal in the microampere to nanoampere range, characterized by small amplitude, high frequency, and challenging measurement requirements. This advancement represents significant progress in micro current detection technology, addressing the limitations of existing methods. Conventional technologies typically have narrow bandwidth and limited dynamic range, which restricts their ability to meet the detection demands of ionization sensors.

#### **4.3.2. Typical disease prevention, bioaerosol database and quantitative analysis methods**

Simulation analysis of bioaerosols in disease prevention, food, and drug safety provides the scientific basis for their direct quantitative analysis. As shown in Figure 4(a), bioaerosol electric field modeling (electric field range:  $0-5\times10^6$  V/m) strongly supports the collection of bioaerosol database samples across food and pharmaceutical applications, which is crucial for preventing the spread of typical diseases. The simulations indicate that a stronger electric field facilitates the release of ionized gas molecules from the negative ion channel. Reducing electrode spacing and

increasing aspect ratio enhance the local electric field, thereby improving ionization efficiency, collector current density, and sensor sensitivity with faster response. However, excessively small electrode spacing increases the risk of electrical breakdown and noise.

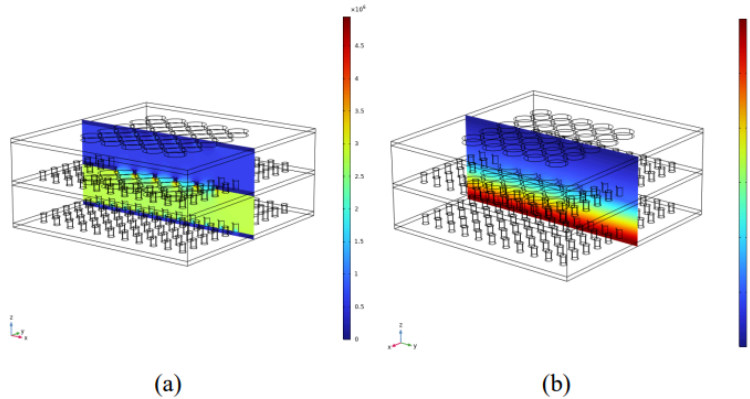


Figure 4. Distribution of (a) the simulated electric field, (b) electric potential

As shown by the preceding electric-field simulation, most existing bioaerosol analysis systems still rely on indirect processing methods for sample collection. Furthermore, electric potential analysis (0–300 V) in Figure 4(b) allows for effective online, real-time detection of aerosol volume concentration. This method outputs both aerosol number concentration and solid mass concentration.

In summary, the modeling based on this approach effectively supports the database and quantitative analysis of bioaerosols relevant to typical disease prevention and food and drug safety.

#### 4.3.3. Effects of electrode spacing and aspect ratio on sensing performance

Simulation studies on the inter electrode spacing revealed that a moderate reduction in spacing enhances the local electric field strength and increases the ion current density. However, excessively small spacing was found to raise the risk of electrical breakdown and elevate noise levels, indicating an optimal range for balancing performance and stability. This finding aligns with recent experimental results on three electrode ionization MEMS sensors. For the silicon micropillar sensor, sensitivity increases with temperature, whereas an increase in bioaerosol particle concentration leads to a reduction in sensitivity. The response of the sensor to different target concentrations was examined over several measurement ranges. At the same time, the sensor also responds to non-target concentrations, and this response varies with changes in non-target levels. For this reason, the cross-sensitivity of the silicon micropillar sensor was analyzed in order to better characterize its overall sensing behavior.

To further elucidate the influence of geometry on sensing performance, simulation results for silicon micropillar structures with low and high aspect ratios were compared. The high aspect ratio structure generates a stronger localized electric field at the pillar tip, significantly improving ionization efficiency and collector current density. In contrast, the low aspect ratio structure shows reduced sensitivity due to a more uniform field distribution. Recent advances in deep reactive ion etching (DRIE) and metal assisted chemical etching (MACE) have enabled the fabrication of high quality, high aspect ratio microstructures with low sidewall roughness over large area silicon wafers.

Furthermore, comparisons of different electrode arrangements and biasing methods show that variations in the inter electrode potential distribution and charge carrier migration paths directly

determine collection efficiency and noise characteristics. Recent studies on three dimensional micropillar sensor electrodes in electrochemistry and ion detection confirm that such sensor designs can effectively suppress random noise and drift error while maintaining high sensitivity.

#### 4.3.4. Correlation between simulation results and aerosol detection performance

Based on the simulation results in Figure 4 outlined earlier, this study builds a quantitative relationship between current density and detection efficiency by mapping current and ion density distributions at the collecting electrode to the collection probability of aerosol particles. The findings show that simultaneous increases in cathode current density, inter electrode positive ion density, and collecting electrode current density can significantly enhance the detection sensitivity and response speed for bioaerosols. Integrating system level design with feature extraction and signal classification through weak AC signal detection and neural network algorithms enables real time identification and digital output of multi parameter bioaerosols. This synergistic optimization of structure, signal, and algorithm provides practical physical and algorithmic support for a high sensitivity, intelligent bioaerosol analyzer.

### 5. Conclusion

The sensor developed in this work is based on a silicon micropillar three-electrode structure and is capable of simultaneously monitoring multiple environmental parameters, including particulate concentration, gas concentration, and temperature. Owing to this design, the sensor can be applied to real-time measurements of bioaerosol concentration, composition, and particle size, providing multi-dimensional information within a single sensing platform. The specific details are described as follows:

1) To better understand the sensing mechanism, Multiphysics simulations were carried out using COMSOL. The analysis focused on how electrode spacing, aspect ratio, and metal film thickness influence the electric field distribution, ion transport, and current density. indicating that the structural parameters must be carefully balanced. In addition, increasing the aspect ratio of the gas channel improves discharge behavior and contributes to higher current density and effective channel density.

2) Sensitivity measurements were then performed using silicon and chromium micropillar sensors with different electrode spacings. The experimental results show that variations in the applied bias voltage directly affect the anode current of the three-electrode sensor. This behavior makes it possible to observe subtle differences in the response patterns of bioaerosol samples and supports the discrimination of different bioaerosol types based on their electrical characteristics. The results also indicate that the sensor is capable of monitoring multiple concentration parameters simultaneously.

Overall, this work presents a practical framework for the direct detection and analysis of bioaerosols using ionization-based MEMS sensors. The study shows that sensor performance is strongly influenced by the combined effects of device geometry, operating conditions, and signal processing methods. These findings improve the understanding of ionization-based sensing and provide guidance for sensor design. They also support the development of integrated and miniaturized systems for real-time environmental monitoring, with applications in disease prevention, food safety, and pharmaceutical quality control.

## References

- [1] Zhang, Y., Wang, C., Xie, L., Peng, Y., & Wang, R. (2024). An Ionization-Based Aerosol Sensor and Its Performance Study. *Sensors*, 24(17), 5600.
- [2] Li, M., Wang, L., Qi, W., et al. (2021). Challenges and perspectives for biosensing of bioaerosol containing pathogenic microorganisms. *Micromachines*, 12(7), 798.
- [3] Iqbal, M. A., Siddiqua, S. A., Faruk, M. O., et al. (2024). Systematic review and meta-analysis of the potential threats to respiratory health from microbial bioaerosol exposures. *Environmental Pollution*, 341, 122972..
- [4] Farrell, A., O'Connor, D., McNamara, K., et al. (2024). Genomic characterization of bioaerosols within livestock facilities: A systematic review. *Science of the Total Environment*, 912, 170722.
- [5] Feng, X., Hu, P., Jin, T., et al. (2024). On-site monitoring of airborne pathogens: Recent advances in bioaerosol collection and rapid detection. *Aerobiologia*, 40, 303–341.
- [6] Mainelis, G. (2020). Bioaerosol sampling: Classical approaches, advances, and perspectives. *Aerosol Science and Technology*, 54(5), 496–519.
- [7] Ma, X., Fang, Z., Li, F., et al. (2020). Determination of performance-parameter design and impact factors of sampling efficiency for bioaerosol cyclones. *Biotechnology and Biotechnological Equipment*, 34(1), 640–651.
- [8] Unigarro, A., & Günther, F. (2025). A comprehensive comparison among capacitive, thermodynamic, and drift-diffusion models for steady-state responses of nanostructured organic electrochemical transistors. *ACS Applied Nano Materials*, 8(23), 12329–12341.
- [9] Shama, Y. S., Rahamanian, S., Mouharrar, H., et al. (2024). Unraveling the nature of sensing in electrostatic MEMS gas sensors. *Microsystems & Nanoengineering*, 10, 56.
- [10] Michaux, E., & Mazouffre, S. (2023). Time-of-Flight Measurements in the Jet of a High-Current Vacuum Arc Thruster. *Aerospace*, 10(12), 1011.
- [11] Zhang, C., Ji, C., Park, Y. B., & Guo, L. J. (2021). Thin-metal-film-based transparent conductors: Material preparation, optical design, and device applications. *Advanced Optical Materials*, 9(3), 2001298.
- [12] Ziae, S., Sarkhosh, M., Saeidi, M., et al. (2025). Public health implications of bacterial and fungal bioaerosol concentrations in outdoor air. *Scientific Reports*, 15, 22706.
- [13] Oeser, L., Samala, N., Hillemann, L., Göhler, D., Müller, J., Jahn-Wolf, C., & Lienig, J. (2024). High-concentration measurements with optical aerosol spectrometers by signal fluctuation analysis. *Journal of Aerosol Science*, 176, 106312.
- [14] Zhu, Y., Fang, T., Verma, V., et al. (2024). Improved calibration strategies for continuous online aerosol measurements and implications for exposure assessment. *Science of the Total Environment*, 908, 168274.
- [15] Hao, W., Stolzenburg, M., Attoui, M., Zhang, J., & Wang, Y. (2021). Optimizing the activation efficiency of sub-3 nm particles in a laminar flow condensation particle counter: Model simulation. *Journal of Aerosol Science*, 158, 105841.